Ocean Sci. Discuss., 6, 1477–1512, 2009
www.ocean-sci-discuss.net/6/1477/2009/

Ocean Science Discussions

Papers published in *Ocean Science Discussions* are under
open-access review for the journal *Ocean Science*

Modelling approach to the assessment of biogenic fluxes at a selected Ross Sea site, Antarctica

M. Vichi[1,2], A. Coluccelli[2,*], M. Ravaioli[3], F. Giglio[3], L. Langone[3], M. Azzaro[4], F. Azzaro[4], R. La Ferla[4], G. Catalano[5], and S. Cozzi[5]

[1]Centro Euro-Mediterraneo per i Cambiamenti Climatici, Bologna, Italy
[2]Istituto Nazionale di Geofisica e Vulcanologia, Bologna, Italy
[3]CNR-ISMAR Sezione di Bologna, Via Gobetti 101, 40129 Bologna, Italy
[4]CNR-IAMC Sezione di Messina, Spianata S. Ranieri 86, 82122 Messina, Italy
[5]CNR-ISMAR Sezione di Trieste, V. le Gessi 2, 34123 Trieste, Italy
[*]now at: Universitá Politecnica delle Marche, Ancona, Italy

Received: 28 May 2009 – Accepted: 29 June 2009 – Published: 8 July 2009

Correspondence to: M. Vichi (vichi@bo.ingv.it)

Published by Copernicus Publications on behalf of the European Geosciences Union.

Abstract

Several biogeochemical data have been collected in the last 10 years of Italian activity in Antarctica (ABIOCLEAR, ROSSMIZE, BIOSESO-I/II). A comprehensive 1-D biogeochemical model was implemented as a tool to link observations with processes and to investigate the mechanisms that regulate the flux of biogenic material through the water column. The model is ideally located at station B (175° E–74° S) and was set up to reproduce the seasonal cycle of phytoplankton and organic matter fluxes as forced by the dominant water column physics over the period 1990–2001. Austral spring-summer bloom conditions are assessed by comparing simulated nutrient drawdown, primary production rates, bacterial respiration and biomass with the available observations. The simulated biogenic fluxes of carbon, nitrogen and silica have been compared with the fluxes derived from sediment traps data. The model reproduces the observed magnitude of the biogenic fluxes, especially those found in the bottom sediment trap, but the peaks are markedly delayed in time. Sensitivity experiments have shown that the characterization of detritus, the choice of the sinking velocity and the degradation rates are crucial for the timing and magnitude of the vertical fluxes. An increase of velocity leads to a shift towards observation but also to an overestimation of the deposition flux which can be counteracted by higher bacterial remineralization rates. Model results suggest that the timing of the observed fluxes depends first and foremost on the timing of surface production and on a combination of size-distribution and quality of the autochtonous biogenic material. It is hypothesized that the bottom sediment trap collects material originated from the rapid sinking of freshly-produced particles and also from the previous year's production period.

1 Introduction

More than 10 years of physical and biogeochemical measurements have been collected in the framework of the Italian Programme for Antarctic Research (PNRA, Pro-

getto Nazionale di Ricerca in Antartide). These data represent a valuable set of information on the dynamical variability of polar ecosystems and can be profitably used to constrain biogeochemical models of the global ocean carbon cycle in the Southern Ocean. On the other hand, models can also be used to support the interpretation of observations, as tools to link data with processes and to investigate the complex mechanisms that regulate the flux of biogenic material through the water column.

We have a fragmented picture of the plankton seasonal cycle in the Ross Sea, mostly derived from composites of diverse biogeochemical data collected in different years (Smith et al., 1996, 2000; Lipizer et al., 2000; Smith and Asper, 2001; Azzaro et al., 2006). Little synoptic observations are available, and the longer seasonal time-series on biogenic components are obtained from sediment trap measurements (Collier et al., 2000; Langone et al., 2000). Phytoplankton growth in the Ross Sea usually initiates in early spring, much earlier than in other regions of the Antarctic, likely because of favourable stratification conditions induced by ice melting (Smith and Asper, 2001). The patchy structure of this process is therefore responsible for the large spatial variability of growth conditions. After the onset of stratification, the spring-summer period is characterized by spatially-extended blooms dominated by diatoms in the north-eastern open water part and by the colonial prymnesiophyte *Phaeocystis Antarctica* in seasonal ice zones and coastal waters (DiTullio et al., 2000; DiTullio and Smith, 1996).

The vertical fluxes of biogenic material are characterized by the occurrence of rapid sinking events (DiTullio et al., 2000; Asper and Smith, 2003; Langone et al., 2003), time-extended small deposition rates that lag the production peak of some months (Gardner et al., 2000; Collier et al., 2000) or by a combination of both phenomena (Langone et al., 2000). It is thus difficult to assess their role in influencing CO_2 fluxes with the atmosphere and the export rates of organic carbon to the deep ocean. Organic fluxes through the water column are apparently a small fraction (5–8%) of the surface production (Langone et al., 2003; Smith and Dunbar, 1998) although moorings located in regions such as the Joides basin (Fig. 1) indicate that deeper deposition rates are more than double the flux collected in shallow trap sediments above (Collier

et al., 2000; Langone et al., 2000). This suggests that processes other than surface export modify the characteristics of the sinking material, the more likely being horizontal advective transport and aggregation mechanisms.

To partly bridge the gaps among these contrasting information, we have implemented a coupled physical-biogeochemical model at station B (175° E–74° S, central Joides basin, Fig. 1) of the PNRA Italian programme, with the aim to reproduce the vertical fluxes of autochtonous organic matter as forced by the dominant water column physics. The ultimate scope of the simulation is thus not to fit the sparse observations, but rather to provide the dynamical framework for hypotheses testing, assessing the model prediction against the available standing stock and rate measurements collected during the Italian and international joint projects (ABIOCLEAR, ROSSMIZE and BIOSESO-I/II). Particularly, this work will focus on the assessment of the vertical fluxes of organic particles and the comparison with data collected in sediment traps. Station B was chosen for several reasons: the more simple physical conditions due to the absence of polynia, a diatom-dominated bloom instead of Phaeocystys (which reduces the complexity of the phytoplankton parameterization) and also because many open questions still remain on the vertical dynamics inferred from sediment traps with respect to other more typical mooring sites (station A, 76.8° S 169° E, Langone et al., 2003)

The next section gives some details on the model features and the interannual forcing functions used to drive the one-dimensional simulation. Section 3 presents model results organized following these major guidelines:

- quantification of the organic matter production in the euphotic layer and comparison with available observations;
- quantification of heterotrophic consumption processes in the mesopelagic layer;
- estimation of model-derived sinking rates at given depths within the aphotic zone;
- comparison with sediment traps data.

Section 3.6 gives an overview of the model sensitivity to the key parameters affecting the vertical fluxes such as sinking velocity and bacterial remineralization rates. The outcomes of the experiments are discussed in Sect. 4 and, finally, Sect. 5 offers some conclusion remarks.

2 The simulation tool

The modelling framework is derived from the system set up by Vichi et al. (2004) to study the open Baltic biogeochemistry. The physical model is a vertical one-dimensional version of the Princeton Ocean Model (Blumberg and Mellor, 1987, POM), where the dynamical core is the turbulence closure scheme proposed by Mellor and Yamada (1982). The total depth of the water column is 588 m and the discrete vertical grid is composed of 30 levels, 5 in the first 20 m with a depth increasing from 1 to 10 m, and the reminder with a constant depth of 22 m.

The Biogeochemical Flux Model (BFM, http://bfm.cmcc.it) was developed as a generalized modelling tool to be coupled to several kind of hydrodynamic models. This model was also applied to the world ocean ecosystem with a global configuration named PELAGOS (PELAgic biogeochemistry for Global Ocean Simulations Vichi et al., 2007a,b). A formal background theory of the model applied to the global ocean is found in Vichi et al. (2007a). The model version used in this application is the standard BFM configuration with the addition of the iron dynamics used in PELAGOS and the further implementation of two forms of sinking organic detritus (cf. Sect. 2.2).

The biogeochemistry model is essentially a biomass-based set of differential equations that allows the simulation of lower trophic levels and major inorganic and organic components of the marine ecosystem. The model is based on the definition of Chemical Functional Families (CFF, Vichi et al., 2007a), which are theoretical constructs representing biogeochemical components in the Eulerian continuum and are further subdivided into living, non-living and inorganic components. Living CFFs are the basis of Living Functional Groups (LFG), the biomass-based functional prototype of the real

organisms. LFGs are grouping of organisms according to their functional behavior in the ecosystem and not to phylogenetic considerations. Both CFFs and LFGs represent the concentrations of measurable properties of marine biogeochemistry such as the carbon content in marine diatoms or the nitrogen contained in dissolved organic matter (Fig. 2). All the model state variables are expressed in terms of time-varying basic components (both elements as C, N, P, Si, O, Fe or biochemical molecules as chl), whose relationships regulate the functioning of a specific LFG (as for instance the chl:C ratio in phytoplankton) or the actual availability (as the nutrient:C ratios in particulate detritus).

As depicted in Fig. 2, the model resolves 4 different LFGs for phytoplankton (diatoms, autotrophic nanoflagellates, picophytoplankton and large phytoplankton), 4 for zooplankton (carnivorous and omnivorous mesozooplankton, microzooplankton and heterotrophic nanoflagellates), 1 LFG for bacteria, 8 inorganic CFFs for nutrients and gases (phosphate, nitrate, ammonium, silicate, dissolved iron, reduction equivalents, oxygen, carbon dioxide) and 11 organic non-living CFFs for dissolved and particulate detritus. With this kind of approach, all the nutrient:carbon ratios in chemical organic and living functional groups, as well as chl:C ratios in phytoplankton, are allowed to vary within their given ranges and each component has a distinct biological and physical time rate of change. This kind of parameterization mimics the acclimation of organisms to the prevailing nutrients and light conditions, and allow the recycling of organic matter to be functionally determined by the actual nutrient content.

2.1 Forcing functions and initial conditions

The model is forced with daily surface fluxes from the ERA40 data set over the period 1990–2001 (Uppala et al., 2005) in a $1^{\circ} \times 1^{\circ}$ degrees region around station B. Daily sea surface temperature (SST) data from the Reynolds data set (Reynolds, 1988) are also used to restore the model SST with a relaxation term of 1 day. This strong nudging rate is needed to parameterize the evolution of the sea ice cover since it is not dynamically computed in the model. Wind stress and downward radiation flux are set to zero when

the computed SST is below the freezing point, while the relaxation term is continuously given to allow the surface to shift from packed-ice to ice-free conditions as typical of this marginal ice zone. During the ice-free conditions the surface restoration term is negligible since the model responds correctly to the surface fluxes.

The model is initialized on 1 June 1990 with average winter temperature, salinity and macronutrient profiles of the whole Ross Sea from the World Ocean Atlas (Conkright et al., 2002). Initial iron concentration is set to $0.25\,\mu\mathrm{mol\,m^{-3}}$ as the average value measured by Sosik and Olson (2002) in the Ross Sea. Biogeochemical LFGs and CFFs are initialized with homogeneous low values mimicking the quiescent winter period. The model is robust to the choice of winter initial conditions for biogeochemical variables in the sense that the difference in the solution trajectories of perturbed experiments (±20%) is limited to less than 5% after one year of simulation.

Nitrate, silicate and phosphate are dynamically relaxed to the background winter profiles with a 3 month time scale when the water column is under packed-ice conditions, parameterizing the replenishment of nutrients caused by non-resolved and three-dimensional advection processes under sea ice.

2.2 Model adaptation

Organic particle dynamics is complex and as a first approximation linked to the constituents and dimensions of particles. The standard BFM configuration assumes that organic detritus can be described by one single class of medium-degradable organic matter with a sinking speed of $1.5\,\mathrm{m\,d^{-1}}$. This is a rough approximation because there is no distinction between denser, fast-sinking detrital material such as faecal pellets and other particulate excretion from smaller heterotrophs, lysis or sloppy feeding products. To differentiate between these groups an additional variable was introduced in the model representing the detritus produced by mesozooplankton (including biogenic silica frustules of grazed diatoms). This CFF ($R_i^{(5)}$ in Fig. 2) has 5 components (C, N, P, Si and Fe) and is assumed to sink with a nominal velocity of $100\,\mathrm{m\,d^{-1}}$. Measurements

in the Ross Sea have in fact reported sinking speeds of organic aggregates of more than $250\,\mathrm{m\,d^{-1}}$ (Asper and Smith, 2003). Sensitivity experiments have been carried out and presented in Sect. 3.6 to analyze the impact of different choices of the organic detritus parameterization on the results.

3 Simulation results

3.1 Water column physics

Figure 3 shows the time-series of the simulated SST, which is mostly controlled by the Reynolds data due to the imposed relaxation constraint. There is a clear interannual variability in the data which is also visible in the atmospheric forcing functions. The maxima in 1992 and 1997 are likely to be related to the large scale variability induced by El Niño, for which correlations have been reported with sea-ice retreat in the Ross Sea (Ledley and Huang, 1997; Kwok and Comiso, 2002).

The long-term vertical structure computed by the model is comparable with the average of the data collected during the deployment and monitoring of the mooring in the 1994–1998 summer campaigns (Fig. 4, Russo et al., 1997). The peculiar dicothermal layer is rather well reproduced by the model. This cold water structure, constrained between the surface warm waters above and the warmer but saltier waters below, is found in the surface layers of high latitude oceans generally between 50 and 150 m depth. Despite a slight discrepancy of 1 model level (22 m) in the location of the minimum, the vertical structure is in good agreement with the available observations, especially in the simulation of the surface mixed layer depth.

3.2 Water column biogeochemistry

The simulated nutrient time-series at the surface are shown in Fig. 5 and compared with the observations from the ROSSMIZE and BIOSESO I campaigns in the station B area

(Catalano et al., unpublished data). Data were collected in December 1994 before the starting of the bloom and during "lower" nutrient concentrations in January 1995 and 1996. Due to the low time resolution of data, it is not possible to infer a clear signal of the exact timing of the bloom. If we assume an ergodic hypothesis in the data distribution, we may say that the model broadly capture the range of the nutrient drawdown. The most remarkable feature is the underestimation of the silicate uptake, which is low even if the simulated bloom is composed of about 60% diatoms and 40% nanoflagellates (not shown) and primary production is comparable with observations as described below. These results are obtained by taking into account an increased Si:C reference ratio of 3 times the standard BFM value due to the effects of Fe limitation (Takeda, 1998; Lancelot et al., 2000), but still the model is not capable of reproducing the observed decrease in silicate concentration.

Autotrophic biomass (as chlorophyll concentration) and gross primary production (GPP) in the euphotic zone over the simulation period are shown in Fig. 6. Station B has a much lower biomass and production rates with respect to the stations in the polynia open waters (Smith et al., 1996, 2000), although the marginal ice zone can reach substantially high production rates and concentrations during the Austral spring (Saggiomo et al., 1998). The model simulates a bulk biomass and GPP rates which are comparable with the available observations (Saggiomo et al., 1998, 2002; Vaillancourt et al., 2003). GPP is highly correlated with SST in the model (r=0.91, p<0.01) and the periods with lower temperatures correspond to the minima of gross production. The chl content is instead less sensitive to temperature values but still significantly correlated (r=0.68, p<0.01). The production peaks are earlier by about one month with respect to the biomass maxima as also observed in the polinya region (Smith et al., 2000). However, in contrast with the latter observations, the model indicates that the maximum of production is in late January–February, and not in December. The nutrient observations are in partial agreement with the model showing a nutrient minima in early February, but the low sampling frequency is not sufficient to corroborate the model results.

Vaillancourt et al. (2003) reported some data on the light regime at station B (station "Sei" of the US-JGOFS programme) during the Austral summer of 1997. The euphotic zone depth was around 40 m and the light diffuse attenuation coefficient was 0.122 m^{-1}. Simulated Chl concentration during this period is lower, and also the chl-specific primary production is about half the reported value of 11 mg C $(mg\,chl)^{-1}\,d^{-1}$. The modeled euphotic zone depth is therefore slightly higher than observed. Furthermore, this diffuse attenuation coefficient is only obtained in the simulation by assuming a background attenuation of 0.08 m^{-1} (about twice the optical attenuation of pure seawater) and a spectrally-integrated chl-specific light absorption of 0.03 $(mg\,chl)^{-1}\,m^2$. The reported values in the polynia region dominated by *Phaeocystis Antarctica* are around 0.01 $(mg\,chl)^{-1}\,m^2$ at the 676 nm red peak (Vaillancourt et al., 2003), but we may assume that a diatom-dominated population can have a larger value due to pigment packaging.

3.3 Phytoplankton light acclimation and growth rates

Several authors have suggested that phytoplankton assemblage in the Ross Sea is adapted to low irradiance and therefore it should not be considered light-limited (Saggiomo et al., 2002; Smith et al., 1996). It is thus important to verify that the model is capable of reproducing these conditions and particularly the low specific growth rates typical of this region (Smith et al., 1999). Figure 7a shows the simulated seasonal evolution in 1996–1998 of the realized chl:C ratio in surface diatoms, superimposed to the optimal value that is used in the model to drive chl synthesis according to the Geider et al. (1996) parameterization. Low chl:C ratios are characteristic of the Ross Sea (Smith et al., 1996). In stations dominated by diatoms, the chl:C ratio was as low as 0.005 (DiTullio and Smith, 1996), which is a value also predicted by the model as the minimum allowed. It is interesting to note that the realized ratio varies less than the potential value because of the water column mixing that homogenizes population adapted to different depths and light conditions.

Figure 7b shows the simulated diatom specific growth rate in the surface layer com-

puted with two different methods: i) estimated from the algebraic sum of the realized specific physiological rates of gross production, rest and activity respiration and activity excretion (cf. Fig. 2); ii) computed from the surface carbon biomass stored every day of simulation and according to the formula used in field estimates (Smith et al., 1999, 2000),

$$\mu = \frac{1}{\Delta t} \ln\left(\frac{C + \Delta C}{C}\right)$$

where C is the biomass concentration and ΔC the biomass change in the sampling interval Δt=1 d. The estimated growth rates of diatoms with the latter method are extremely low during the summer season, generally around 0.1 d^{-1} (Smith et al., 1999, 2000). The model agrees well with these estimates, implying that the net carbon production rates are reasonably simulated. However, these values are achieved only by applying a 0.5 coefficient to the non dimensional temperature regulating factor of phytoplankton growth based on the Q10 function (Vichi et al., 2007a). Indeed, Smith et al. (1999) suggested that the maximum growth rates predicted by temperature-dependent exponential models could overestimate growth at temperature lower than 2°C. Goldman and Carpenter (1974) values are in fact about half the ones parameterized with the Eppley curve. Model results also suggest that the choice of the method can lead to different values. The thick line in fact represents the growth induced by local light and nutrient conditions, as the one obtained from controlled on-deck incubations. It is also visible a decrease during the maximum productive periods due to self-shading effects. The thin line is instead the realized change of mass due to a combination of physiological processes, vertical mixing and grazing rates. This is more similar to what can be measured in-situ, and is less representative of the physiological state of phytoplankton.

3.4 Microbial respiration

Scarce information are available on the oxidation of organic matter in the mesopelagic layer of the Ross Sea. A recent work by Azzaro et al. (2006) provides the first estimates

of microbial respiration in the aphotic zone, pointing out that about 63% of the organic carbon remineralized by respiration is derived from the detrital pool. Indeed, the model predict a very low concentration of DOC due to the excess of macronutrient availability, which reduces the release of polysaccharides from nutrient-limited autotrophic cells.

We have used the estimates of Azzaro et al. (2006) to assess the capability of the model to reproduce the remineralization of organic matter in the mesopelagic layer. Figure 8 shows the simulated vertical distribution of microbial biomass and respiration rate during the period of the 2001 BIOSESO II campaign. The depth-integrated value of microbial biomass at site B in the mesopelagic layer (100–600 m), estimated from the measured ATP, varied from 480 to 840 mg C m^{-2}, and the depth-integrated respiration-derived carbon flux, calculated from direct ETS measurements, was 17.3 mg C m^{-2} d^{-1}. Both in the pre-bloom and bloom conditions (mid January and late February, respectively), the model shows a surface maximum of microbial respiration, with small subsurface maxima at 500 m. Microbial biomass shows the same pattern in January, with a relative maximum in the deeper part. In February, the larger amount of freshly produced particles allows microorganisms to homogeneously distribute over the whole water column, but still showing the maximum at 500 m. Microbial respiration eventually increases during late summer-autumn, following the bulk of organic matter produced in the euphotic zone that reaches this depth in April–May (cf. sections below). Integrated values agree with the available observations, implying that the bulk of the remineralization process is rather well captured by the model.

3.5 Simulated sediment trap fluxes

Fluxes at the depths of the real sediment trap locations were computed as the product of the prognostic detritus concentrations at the selected depths with the respective sinking velocity. Figure 9 shows the comparison of model results with the fluxes estimated in the bottom-tethered trap at about 550 m (Langone et al., 2000) for organic C, N and biogenic silica (BSi). The peaks of the simulated fluxes are delayed by about 2 months with respect to the observations. Simulated maxima are quasi-simultaneous

with the surface peaks in the modeled biomass, as indicated by the triangles in the upper axes of each subplot. This implies that the occurrence of the peak in the simulated trap is linked to the timing of the bloom in the model, which is in turn linearly correlated with the SST.

On the other hand, the amplitude of the simulated C flux is in good agreement with the observations, and also the increase between 1995 and 1996, which is explained by the model as a response to the changes in SST and surface primary production. The fluxes of organic N closely follow the time distribution both in the data and in the model, but are overestimated by a factor 2–3. BSi is instead underestimated with respect to the trap data, which is likely to be related to the low consumption of dissolved silicate in the surface layers (Fig. 5).

The simulated deposition flux can be separated in the components due to the fast-sinking detritus produced by mesozooplankton and to the slow-sinking detritus for the surface and bottom traps (Fig. 10, for the C component only). In contrast with the observations (Langone et al., 2000), the peak in the top trap (Fig. 10a) is higher than the bottom trap during the productive phase and is mostly composed of large fast-sinking particles. The maximum of slow detritus is simulated in middle winter, with a lag of about 3 months with respect to the surface production peak as also found in other sediment trap data (Collier et al., 2000). The bottom trap (Fig. 10b) is instead characterized by a summer peak mostly composed of slow detritus produced in the year before. This is followed by the peak of freshly-produced organic matter that sinks down with a velocity of $100\,\mathrm{m\,d^{-1}}$ and reaches the bottom trap almost at the same time of the trap above. It is interesting to note that there are periods such as late-spring and early-summer in which the bottom trap simulated flux is larger than the one above as also found in the observations (Langone et al., 2000).

3.6 Sensitivity analysis

The results shown in the previous sections have been obtained after a set of sensitivity analysis on the types of simulated detritus and their respective sinking and degradation rates. Table 1 reports the experiments that have been performed and the effects on the simulated vertical carbon fluxes at the sediment traps are depicted in Fig. 11. Experiment D0 is the standard BFM setup with one single type of detritus $R^{(6)}$ (Fig. 2); experiment D5 is the reference simulation run that has been previously described.

The difference between D0 and D1 shows the effect of the addition of another detrital component, $R^{(5)}$. With one slow-sinking detritus, the flux at the top trap is composed of one single peak that lags by 4 months the maximum of surface biomass and by 5 months the maximum of production. In D1, the addition of a relatively fast-sinking ($10\,\mathrm{m\,d^{-1}}$) component produced by the diatom grazers shifts the surface peak towards the bloom period and reduces the winter maximum. The same also occurs to a lesser extent in the bottom trap. The choice of the degradation rate of $R^{(5)}$ detritus determines the amplitude of the summer peak. In run D2 the rate is decreased of 1 order of magnitude, while in D3 is set to $0.5\,\mathrm{d^{-1}}$, equivalent to the availability of freshly-produced DOM. It is important to remember that these coefficients represent the availability of substrate to bacteria. Part of the substrate available to bacteria is converted to CO_2 and biomass in the model, but a fraction of it is also moved to the slow-sinking and less degradable compartment simulating a decrease of the organic matter quality. When the degradation rate is slow as in D2, more $R^{(5)}$ reaches both traps; when, conversely, the rate is higher as in D3 and the sinking rate is still $10\,\mathrm{m\,d^{-1}}$, almost no fast-sinking detritus is found.

Setting the sinking rate to $100\,\mathrm{m\,d^{-1}}$(run D4 and D5) shifts the deposition maxima towards the timing of the surface bloom but also lead to an overestimation of the deposition rates at both traps with respect to the observations. Only by assuming a large availability of $R^{(5)}$ as in D5, the reference simulation, it is possible to obtain simulated fluxes which are comparable with the data. Noteworthily, and despite the large overestimation, run D4 shows a larger flux in the bottom trap with respect to the one above, as also observed in data from station B moorings (Langone et al., 2000; Collier et al., 2000).

4 Discussion

The material collected in sediment traps is the result of a dynamical balance between the net export rate due to euphotic production, and the degradation and sinking rates, which are mostly determined by the size and quality of the particles. All these processes occur simultaneously in the upper ocean, and thus the estimation of vertical fluxes by means of surface sediment traps is affected by several biases (Buesseler, 1991, 1998; Smith and Dunbar, 1998). The use of numerical models is a possible methodology to support the assessment of the organic matter fate in the deep ocean, particularly in key regions like the Southern Ocean where the collection of long term time-series is limited. Within the limits of the one-dimensional assumption, the production of organic matter in the upper ocean was simulated as a function of physical conditions, light and nutrient availability, and the prognostic vertical flux of organic material at selected depths was used to compare with deep-ocean sediment traps. Comprehensive biogeochemical models like the BFM can provide some of the dynamical linkages between observations derived from multidisciplinary campaigns. However, biogeochemical models need to be applied with due attention, because of the many assumptions in the parameterization of physiological and ecological processes (Vichi et al., 2007a).

The BFM has many parameters which can be adjusted to reproduce the observed biogeochemical system behaviour. Data constraints in the Ross Sea region are limited and therefore a complete model tuning is not feasible. Since the model was mostly developed for temperate regions, we have performed a set of classical sensitivity analysis to identify the parameters which affect the biogeochemical processes under high latitude environmental conditions. The key parameters affecting the succession of phytoplankton groups are the basal respiration rates which determine the survival standing stock during wintertime. For this purpose, the standard BFM values have been halved for all the functional groups. This implies the need to refine the parameterization of vegetative stages, in order to compute the high initial growth rates measured in labo-

ratory experiments of light deprivation when phytoplankton is brought back to sufficient irradiance levels after a dark period of several months (Peters and Thomas, 1996). The choice of the same respiration rate for diatoms and flagellates was necessary to obtain a dominance of diatoms but also a sufficient abundance of nanoflagellates, as observed in the station B area (Saggiomo et al., 2002).

Other important parameters are the availability coefficients of phytoplankton to grazers. Both grazing and iron are factors limiting the diatom bloom in the model. If iron limitation is deactivated in the model, the bloom is much larger and the time duration is totally controlled by grazing. The sensitivity of the model to grazing coefficients is rather high, particularly because the over-wintering biomass is small and an excessive grazing pressure can completely deplete one of the phytoplankton group. This is for example the case of the simulated eukaryotic picophytoplankton, which is overgrazed by heterotrophic nanoflagellates living on bacteria. Nevertheless, it is difficult to assess the ecological relevance of this component (Vanucci and Bruni, 1998) and therefore we assumed that the microbial loop is limited to bacteria and their grazers. Bacterial biomass in the model is indeed strongly related to the predation pressure by heterotrophic nanoflagellates (HNAN). Synoptic measurements of bacterial activity and HNAN biomass (e.g. Vanucci and Bruni, 1999) are thus needed to achieve a larger confidence in the microbial activity rates produced by the model in the mesopelagic layer.

The physical evolution of the water column simulated by the model and shown in Sect. 3.1 is sufficient to provide the major physical mechanisms typical of this region. However, marginal ice zones are affected by a large degree of spatial variability and local physical conditions can be very different depending on the sea-ice distribution. We cannot expect the model to reproduce this variability, and particularly the Austral spring conditions where biogeochemical samples are collected in leads or in the wakes of the research vessels (Saggiomo et al., 1998). This implies that a lag of 1 or even 2 months in the evolution of the simulated phytoplankton bloom is likely to be ascribed to the forcing functions which are derived from low resolution datasets.

Although the timing of the bloom is difficult to be captured by the model, the estimate of gross primary production and autotrophic chl-based biomass are in reasonable agreement with the available observations (Sect. 3.2). Phosphorus and nitrate drawdown are also within the observed ranges. The comparison with bottom traps, however, reveals some deficiencies in the simulation of organic matter utilization in the mesopelagic layer. Simulated microbial carbon consumption rates match the data (cf. Sect. 3.4) but probably the nutrient utilization rates need to be further verified. The organic N flux at the bottom trap is in fact overestimated by the model, leading to a C:N ratio which is about half the observed. The C:N ratios in simulated sinking detritus is a function of the actual ratio in the functional group that produces it. Since phytoplankton is allowed to uptake nutrients up to twice the optimal ratio (set to Redfield, Vichi et al., 2007a), the particulate derived from phytoplankton would have the same ratio unless nutrients are stripped from the organic matter by heterotrophic degradation. Modeled bacteria extract nutrients from the organic matter according to their requirements (Goldman et al., 1987), which are closer to the ratios found in the organic matter produced by nutrient-replete phytoplankton. It is therefore important to further verify the model parameterization of N uptake, comparing it with the available information on isotopic N uptake experiments (e.g. Lipizer et al., 2000; Cochlan and Bronk, 2001).

Silicate consumption in the surface layer is clearly underestimated with respect to the available data (Fig. 5). This is also confirmed by the underestimation of the BSi fluxes at the bottom trap (Fig. 9c). It is known that diatoms requires larger amount of silica in iron-depleted conditions (Takeda, 1998), but apparently even a 3 times higher Si:C ratio is not sufficient to reproduce the observations. In a model of the Kerguelen region, Pondaven et al. (2000) had to artificially increase this ratio up to 5 times to reproduce the observed silicate concentrations. The specific dissolution rate of BSi used in the model is already in the lower range of the measured rates in the Southern ocean (Treguer et al., 1989, 0.01 d^{-1}), therefore the cause of this discrepancy is likely to be ascribed to the silica storage in diatom frustules and the relationships with iron utilization and sinking rates which are still largely unknown.

Carbon production rates of diatoms are indeed in the range of the observed values as shown in Fig. 7. Model results also indirectly demonstrate how the physics may affect the physiological rate of phytoplankton and how different can be the estimates derived from standing stock measurements. The realized chl:C ratios are in fact always less varying than the theoretical value predicted by the Geider et al. (1996) parameterization, implying that the light-acclimation and the response to light of the average mixed layer population is different from the one derived from simpler parameterizations of light-limited growth. Models such as the BFM that takes into account these acclimation processes are therefore needed to appropriately capture this behavior.

The sensitivity analyses on detritus parameterization presented in Sect. 3.6 suggest that by varying the dimension and quality of the detrital particles we can obtain several patterns of vertical fluxes that have been actually observed in the Ross Sea sediment traps (DiTullio et al., 2000; Langone et al., 2000; Collier et al., 2000; Gardner et al., 2000; Langone et al., 2003; Asper and Smith, 2003). The succession of different phytoplankton groups is an important factor that contributes to the size-distribution and quality of organic detritus formed in the euphotic layer. The diatom dominance and the presence of nanoflagellates at station B lead to the concurrent production of larger and smaller particles that are likely to be the cause of the different deposition rates observed in the top and bottom traps. It can be hypothesized that the organic matter collected in the surface trap is directly related to the surface production, which is by nature subjected to the highly variable atmospheric and sea-ice conditions. The bottom trap, on the other hand, collects both freshly-produced fast-sinking particles but also degraded slow-sinking material derived from the previous seasonal production phase. This detritus is accumulated throughout the year in the mesopelagic layer and the deposition flux is also probably modulated by three-dimensional advective processes, topographic features (Langone et al., 2000) and particle aggregation (Asper and Smith, 2003).

The timing of the bloom and of the deposition maxima are a major discrepancy in the comparison between trap data and simulation results. Apparently, the bloom at station B starts very early, already under packed ice conditions (Saggiomo et al., 1998)

and the model cannot reproduce this feature. It is expected that the implementation of a sea ice biogeochemistry model as the one developed by Tedesco et al. (2009) would improve the results, explaining further the possible biological mechanisms of this delay. In addition, the fluxes in the top sediment trap suggest that there is a rapid decay of the bloom, which was not possible to simulate in the model with the current parameterization of grazers. We might also hypothesize that the bloom does not progress beyond January because of the presence of efficient predators which are not resolved in the model. Saggiomo et al. (1998) have reported the presence of krill attached to the ice fragments during the 1994 spring cruise which might exert a substantial control on the development of larger phytoplankton.

5 Conclusions

The Southern Ocean, and particularly the ocean regions around Antarctica are characterized by prolonged summer phytoplankton blooms that are visible in ocean color satellite images. The implications for the global ocean carbon cycle are substantial, but the description of biogeochemical processes in these regions is still rather sketchy.

This work is a first approach to link the various kind of data collected during the Italian expeditions in the Ross Sea, in order to provide an overview of the mechanisms regulating the export of organic material to the ocean floor. The one-dimensional implementation obviously neglects the contributions of advective fluxes. However, this approach allowed to separate the contribution of local biogeochemical processes and to identify how much of the observed variability can be explained by vertical dynamics only. The model can explain some of the patterns observed in the sediment traps, connecting it to production and consumption rates of the organic matter that have been compared with the available measurements. However, it is still to be demonstrated whether the model predictions on export rates can be extrapolated to the whole Ross Sea, and particularly to the polinya regions dominated by the colonial *Phaeocystis Antarctica*.

The results of the modelling experiments suggest the need of a more comprehensive collection of biogeochemical rate measurements associable with the sediment trap time-series. In particular, the nature and composition of the sinking organic matter should be accurately estimated in order to improve the implemented parameterizations and verify the possibility of multi-year accumulation of organic matter as suggested by the model. The availability of multivariate observations can lead to a more effective use of this modelling tool to better understand the processes involved in the Ross Sea carbon export dynamics.

Acknowledgements. This research was supported by the Italian projects BIOSESO I and II of the Progetto Nazionale di Ricerca in Antartide and by the Italian FISR project VECTOR.

References

Asper, V. L. and Smith, W. O.: Abundance, distribution and sinking rates of aggregates in the Ross Sea, antarctica, Deep-Sea Res. II, 50, 131–150, 2003. 1479, 1484, 1494

Azzaro, M., La Ferla, R., and Azzaro, F.: Microbial respiration in the aphotic zone of the Ross Sea (antarctica), Mar. Chem., 99, 199–209, 2006. 1479, 1487, 1488, 1509

Blumberg, A. and Mellor, G.: A description of a three-dimensional coastal ocean circulation model, in: Three-dimensional coastal ocean model, edited by: Heaps, N., American Geophysical Union, 1–16, 1987. 1481

Buesseler, K. O.: Do upper-ocean sediment traps provide an accurate record of particle-flux?, Nature, 353, 420–423, 1991. 1491

Buesseler, K. O.: The decoupling of production and particulate export in the surface ocean, Global Biogeochem. Cy., 12, 297–310, 1998. 1491

Cochlan, W. P. and Bronk, D. A.: Nitrogen uptake kinetics in the Ross Sea, Antarctica, Deep Sea Res. II, 48, 4127–4153, 2001. 1493

Collier, R., Dymond, J., Honjo, S., Manganini, S., Francois, R., and Dunbar, R.: The vertical flux of biogenic and lithogenic material in the Ross Sea: moored sediment trap observations 1996–1998, Deep Sea Res. II, 47, 3491–3520, 2000. 1479, 1489, 1490, 1494

Conkright, M., Garcia, H., O'Brien, T., Locarnini, R., Boyer, T., Stephens, C., and Antonov, J.: World Ocean Atlas 2001, Volume 4: Nutrients. Vol. NOAA Atlas NESDIS 52, US Govern-

ment Printing Office, Washington DC, cD-ROMs, http://www.nodc.noaa.gov/OC5/WOA01/woa01v4d.pdf, 2002. 1483

DiTullio, G. R., Grebmeier, J. M., Arrigo, K. R., Lizotte, M. P., Robinson, D. H., Leventer, A., Barry, J. P., VanWoert, M. L., and Dunbar, R. B.: Rapid and early export of Phaeocystis antarctica blooms in the Ross Sea, Antractica, Nature, 404, 595–598, 2000. 1479, 1494

DiTullio, G. R. and Smith, W. O.: Spatial patterns in phytoplankton biomass and pigment distributions in the Ross sea, J. Geophys. Res., 101, 18467–18477, 1996. 1479, 1486

Gardner, W. D., Richardson, M. J., and Smith, W. O.: Seasonal patterns of water column particulate organic carbon and fluxes in the Ross Sea, Antarctica, Deep Sea Res. II, 47, 3423–3449, 2000.. 1479, 1494

Geider, R., MacIntyre, H., and Kana, T.: A dynamic model of photoadaptation in phytoplankton, Limnol. Oceanogr., 41(1), 1–15, 1996. 1486, 1494

Goldman, J., Caron, D., and Dennet, M.: Regulation of gross growth efficiency and ammonium regeneration in bacteria by substrate C:N ratio, Limnol. Oceanogr., 32(6), 1239–1252, 1987. 1493

Goldman, J. C. and Carpenter, E. J.: A kinetic approach to the. effect of temperature on algal growth, Limnol. Oceanogr., 19, 756–766, 1974. 1487

Kwok, R. and Comiso, J. C.: Southern Ocean climate and sea ice anomalies associated with the Southern oscillation, J. Climate, 15, 487–501, 2002. 1484

Lancelot, C., Hannon, E., Becquevort, S., Veth, C., and De Baar, H.: Modeling phytoplankton blooms and carbon export production in the Southern Ocean: dominant controls by light and iron in the Atlantic sector in Austral spring 1992, Deep-Sea Res. II, 47(9), 1621–1662, 2000. 1485

Langone, L., Dunbar, R. B., Mucciarone, D. A., Ravaioli, M., Meloni, R., and Nittrouerand, C. A.: Rapid sinking of biogenic material during the late austral summer in the Ross Sea, Antarctica, in: Biogeochemistry of the Ross Sea, edited by: DiTullio, G. and Dunbar, R., Vol. 78 of Antarctic Research Series Monograph, American Geophysical Union, 221–234, 2003. 1479, 1480, 1494

Langone, L., Frignani, M., Ravaioli, M., and Bianchi, C.: Particle fluxes and biogeochemical processes in an area influenced by seasonal retreat of the ice margin (northwestern Ross Sea Atarctica), J. Marine Syst., 27, 221–234, 2000. 1479, 1480, 1488, 1489, 1490, 1494

Ledley, T. S. and Huang, Z.: A possible ENSO signal in the Ross sea, Geophys. Res. Lett., 24, 3253–3256, 1997. 1484

Lipizer, M., Mangoni, O., Catalano, G., and Saggiomo, V.: Phytoplankton uptake of ^{15}N and ^{14}C in the Ross Sea during austral spring 1994, Polar Biol., 23, 495–502, 2000. 1479, 1493

Mellor, G. and Yamada, T.: Development of a Turbulence Closure Model for Geophysical Fluid Problems, Rev. Geophys. Space Phys., 20(4), 851–875, 1982. 1481

Peters, E. and Thomas, D. N.: Prolonged darkness and diatom mortality I: Marine Antarctic species, J. Exp. Mar. Biol. Ecol., 207, 25–41, 1996. 1492

Pondaven, P., Ruiz-pino, D., Fravalo, C., Treguer, P., and Jeandel, C.: Interannual variability of Si and N cycles at the time-series station KERFIX between 1990 and 1995 – A 1-D modelling study, Deep-Sea Res. I, 47, 223–257, 2000. 1493

Reynolds, R.: A real-time global sea surface temperature analysis, J. Climate, 1, 75–86, 1988. 1482

Russo, A., Gallarato, A., Testa, G., Corbo, C., and Pariante, M.: Physical data collected during ROSSMIZE cruise (Ross sea, November–December 1994), in: ROSSMIZE (Ross Sea Marginal Ice Zone Ecology) data report 1993-1995, Part I, edited by: Faranda, F., Guglielmo, L., and Povero, P., Nat. Prog. Ant. Res., 25–110, 1997. 1484

Saggiomo, V., Carrada, G. C., Mangoni, O., d'Alcalá, M. R., and Russo, A.: Spatial and temporal variability of size-fractioned biomass and primary production in the Ross Sea (Antarctica) during austral spring and summer, J. Marine Syst., 17, 115–127, 1998. 1485, 1492, 1494, 1495, 1507

Saggiomo, V., Catalano, G., Mangoni, O., Budillon, G., and Carrada, G. C.: Primary production processes in ice-free waters of the Ross Sea (Antarctica) during the austral summer 1996, Deep Sea Res. II, 49, 1787–1801, 2002. 1485, 1486, 1492, 1507

Smith, W. O. and Asper, V. L.: The influence of phytoplankton assemblage composition on biogeochemical characteristics and cycles in the southern Ross Sea, Antarctica, Deep Sea Res. I, 48, 137–161, 2001. 1479

Smith, W. O. and Dunbar, R. B.: The relationship between new production and vertical flux on the Ross Sea continental shelf, J. Marine Syst., 17, 445–457, 1998. 1479, 1491

Smith, W. O., Marra, J., Hiscock, M. R., and Barber, R. T.: The seasonal cycle of phytoplankton biomass and primary productivity in the Ross Sea, Antarctica, Deep Sea Res. II, 47, 3119–3140, 2000. 1479, 1485, 1487

Smith, W. O., M.Nelson, D., and Mathot, S.: Phytoplankton growth rates in the Ross Sea, Antarctica, determined by independent methods: temporal variations, J. Plankton Res., 21(8), 1519–1536, 1999. 1486, 1487

Smith, W. O., Nelson, D. M., DiTullio, G. R., and Leventer, A. R.: Temporal and spatial patterns in the Ross Sea: phytoplankton biomass, elemental composition, productivity and growth rates, J. Geophys. Res., 101(C8), 18455–18465, 1996. 1479, 1485, 1486

Sosik, H. M. and Olson, R. J.: Phytoplankton and iron limitation of photosynthetic efficiency in the Southern Ocean during late summer, Deep Sea Res. I, 49, 1195–1216, 2002. 1483

Takeda, S.: Influence of iron availability on nutrient consumption ratio of diatoms in oceanic waters, Nature, 393, 774–777, 1998. 1485, 1493

Tedesco, L., Vichi, M., Haapala, J., and Stipa, T.: On the relevance of a dynamic biologically-active layer for numerical studies of the sea ice ecosystem, Ocean Modell., submitted, 2009. 1495

Treguer, P., Kamatani, A., Gueneley, S., and Queguiner, B.: Kinetics of dissolution of antarctic diatom frustules and the biogeochemical cycle of silicon in the Southern Ocean, Polar Biol., 9, 397–403, 1989. 1493

Uppala, S., Kallberg, P., Simmons, A., Andrae, U., da Costa Bechtold, V., Fiorino, M., Gibson, J., Haseler, J., Hernandez, A., Kelly, G., Li, X., Onogi, K., Saarinen, S., Sokka, N., Allan, R., Andersson, E., Arpe, K., Balmaseda, M., Beljaars, A., van de Berg, L., Bidlot, J., Bormann, N., Caires, S., Chevallier, F., Dethof, A., Dragosavac, M., Fisher, M., Fuentes, M., Hagemann, S., Holm, E., Hoskins, B., Isaksen, L., Janssen, P., Jenne, R., McNally, A., Mahfouf, J.-F., Morcrette, J.-J., Rayner, N., Saunders, R., Simon, P., Sterl, A., Trenberth, K., Untch, A., Vasiljevic, D., Viterbo, P., and Woollen, J.: The era-40 re-analysis, Q. J. Roy. Meteorol. Soc., 131, 2961–3012, doi:10.1256/qj.04.17, 2005. 1482

Vaillancourt, R. D., Marra, J., Barber, R. T., and Smith, W. O.: Primary productivity and in situ quantum yields in the Ross Sea and Pacific Sector of the Antarctic Circumpolar Current, Deep Sea Res. II, 50, 559–578, 2003. 1485, 1486, 1507

Vanucci, S. and Bruni, V.: Presence or absence of picophytoplankton in the western ross sea during spring 1994: a matter of size definition?, Polar Biol., 20, 9–13, 1998. 1492

Vanucci, S. and Bruni, V.: Small nanoplankton and bacteria in the Western Ross Sea during sea-ice retreat (spring 1994), Polar Biol., 22, 311–321, 1999. 1492

Vichi, M., Masina, S., and Navarra, A.: A generalized model of pelagic biogeochemistry for the global ocean ecosystem. Part II: numerical simulations, J. Marine Syst., 64, 110–134, 2007a. 1481

Vichi, M., Pinardi, N., and Masina, S.: A generalized model of pelagic biogeochemistry for the global ocean ecosystem. Part I: theory, J. Marine Syst., 64, 89–109, 2007b. 1481, 1487, 1491, 1493

Vichi, M., Ruardij, P., and Baretta, J. W.: Link or sink: a modelling interpretation of the open Baltic biogeochemistry, Biogeosciences, 1, 79–100, 2004, http://www.biogeosciences.net/1/79/2004/. 1481

Table 1. List of sensitivity experiments on the detritus sinking and degradation rates. $R^{(5)}$ and $R^{(6)}$ are the fast- and slow-sinking components of detritus, respectively (cf. Fig. 2). D5 is the reference simulation shown in Sect. 3.

	D0	D1	D2	D3	D4	D5
Number of DET variables	1	2	2	2	2	2
$R^{(5)}$ sinking rate ($m\,d^{-1}$)	–	10	10	10	100	100
$R^{(6)}$ sinking rate ($m\,d^{-1}$)	1.5	1.5	1.5	1.5	1.5	1.5
$R^{(5)}$ degradation rate (d^{-1})	–	0.1	0.01	0.5	0.01	0.5
$R^{(6)}$ degradation rate (d^{-1})	0.01	0.01	0.01	0.01	0.01	0.01

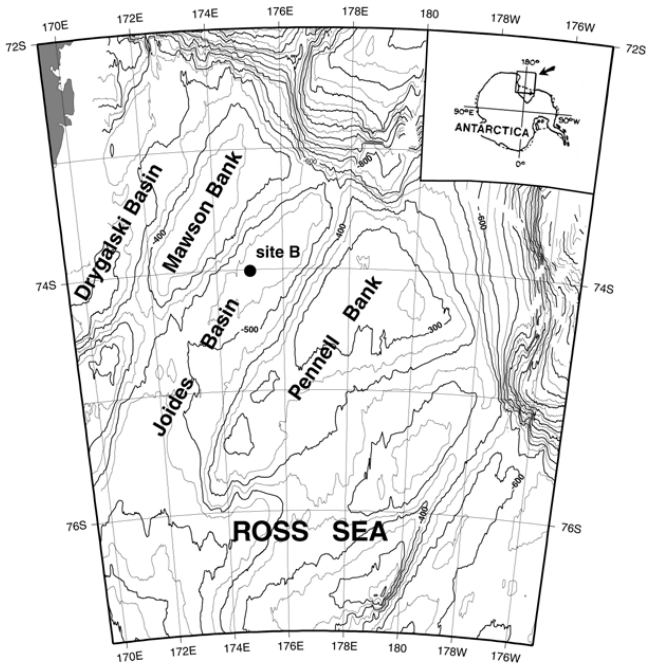

Fig. 1. Map showing the location of station B and the bathymetry of the Ross Sea (depths are in m).

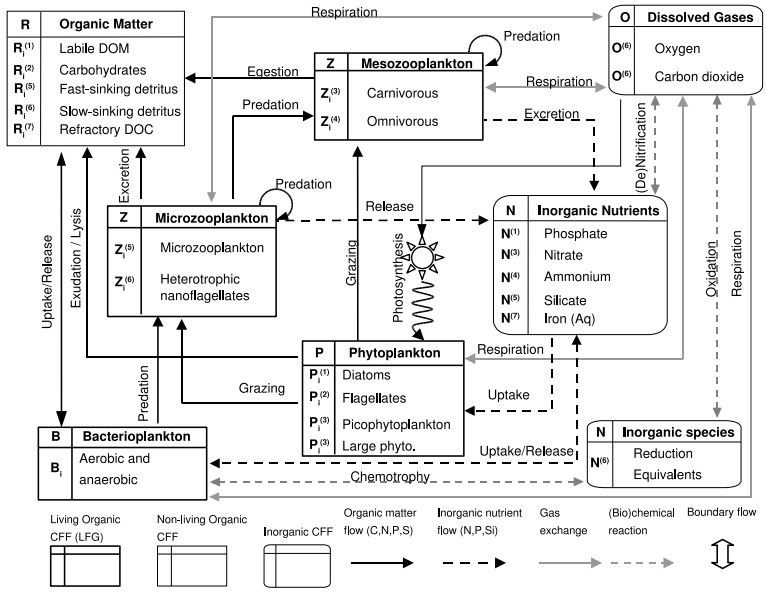

Fig. 2. Scheme of the pelagic BFM model with state variables divided in living, non-living and inorganic Chemical Functional Families. The arrows represent the exchanges of inorganic and organic matter according to the major physiological and ecological processes.

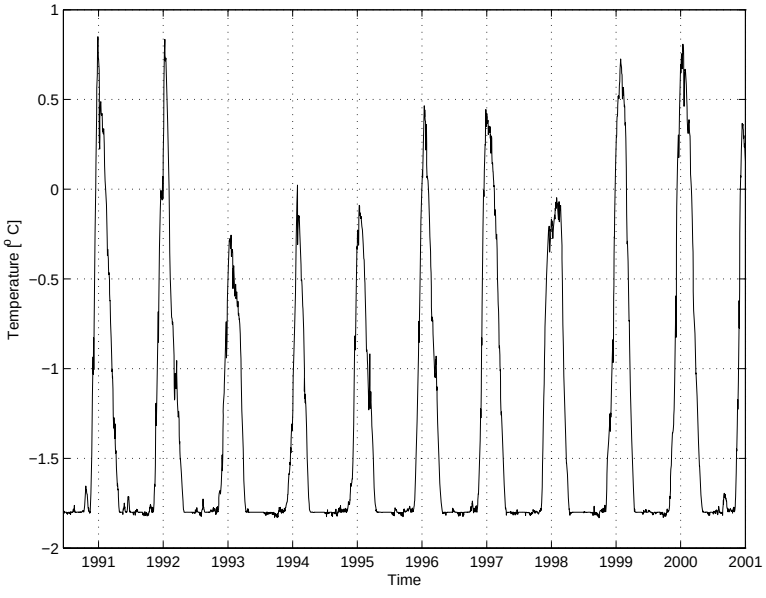

Fig. 3. Time-series of simulated sea surface temperature at station B.

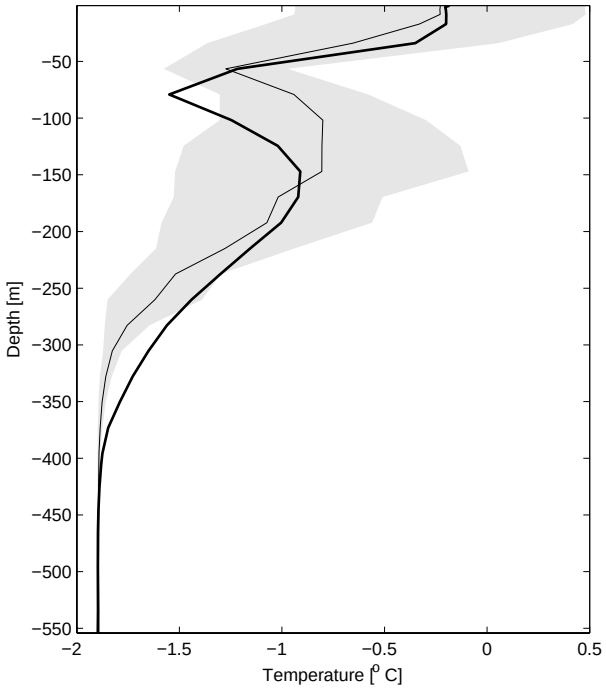

Fig. 4. Simulated (thick line) and observed (dashed line plus standard deviation in gray shading) temperature profile at station B over the period 1995–1998. Data have been interpolated to the model levels.

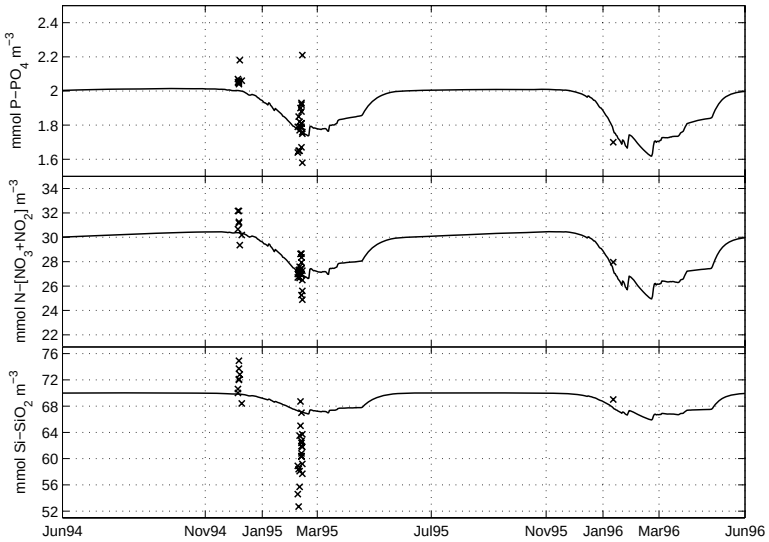

Fig. 5. Simulated (continuous line) and observed (crosses) concentrations of dissolved macronutrients at station B: **(a)** phosphate, **(b)** nitrate + nitrite, **(c)** silicate.

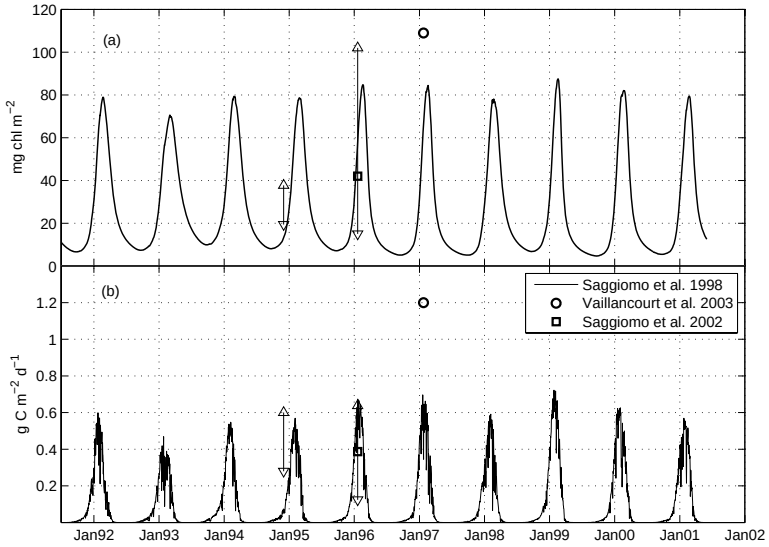

Fig. 6. **(a)** Simulated phytoplankton chlorophyll and **(b)** gross primary production integrated over the first 100 m. Data and ranges of variability from Saggiomo et al. (1998, 2002); Vaillancourt et al. (2003) are indicated as reference for the station B area.

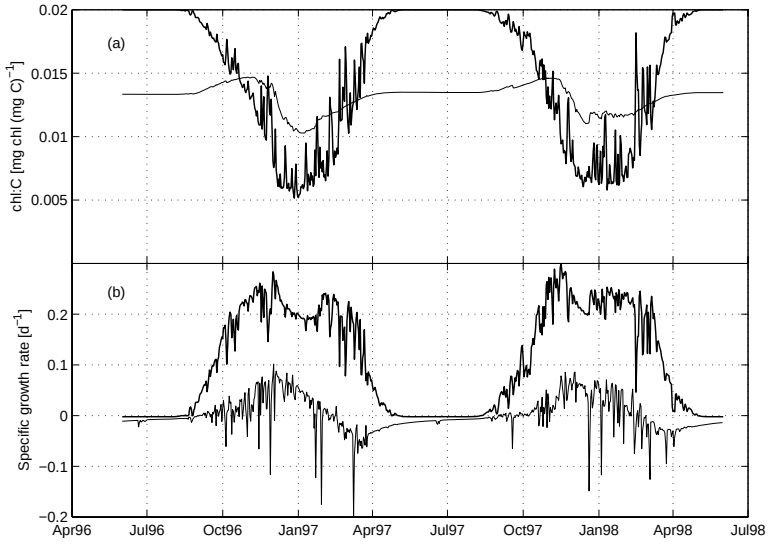

Fig. 7. **(a)** Simulated chl:C ratio in surface diatoms. Thick line: potential theoretical ratio; thin line: realized ratio. **(b)** Simulated specific growth rate of surface diatoms. Thick line: computed as photosynthesis – respiration – excretion; thin line: estimated from carbon biomass concentration.

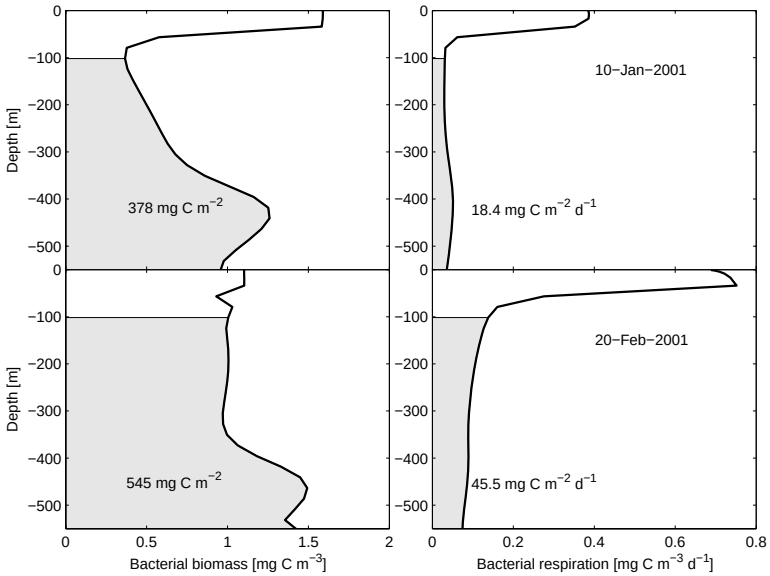

Fig. 8. Simulated profiles of bacterial biomass and respiration rates on 10 January 2001 (top panels) and 20 February 2001 (bottom panels). Integrated values in the mesopelagic layer (shaded area) are also given for comparison with observations (Azzaro et al., 2006).

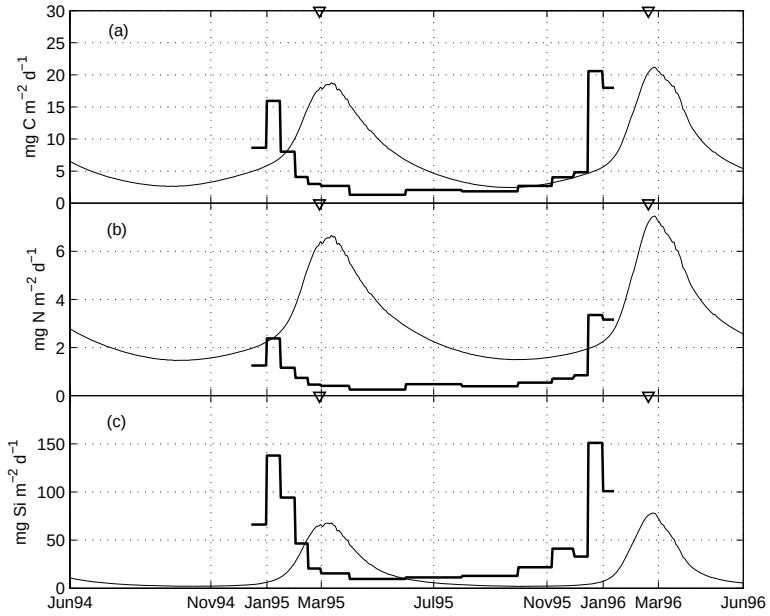

Fig. 9. Observed (thick line) and simulated organic matter fluxes at the bottom sediment trap (550 m) for **(a)** organic C, **(b)** organic N and (b) biogenic Si. The triangles mark the occurrences of the surface biomass peaks in 1995 and 1996.

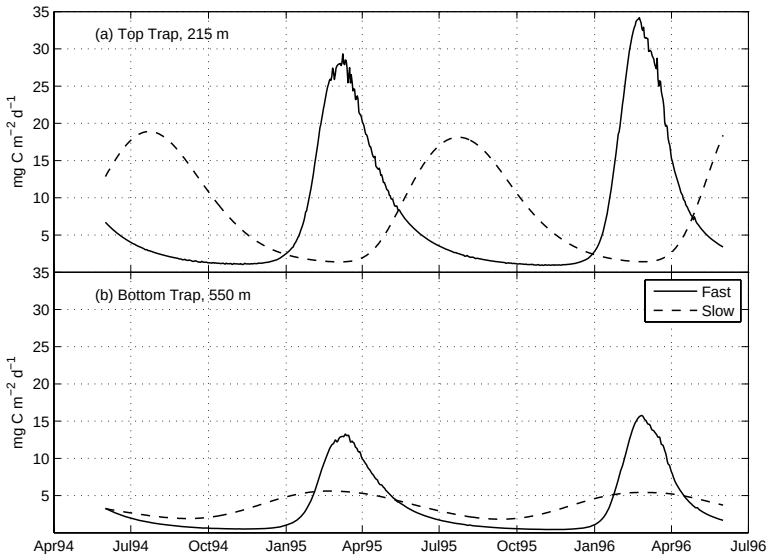

Fig. 10. Contribution of the two types of detritus to the simulated organic carbon fluxes in the **(a)** top and **(b)** bottom sediment traps.

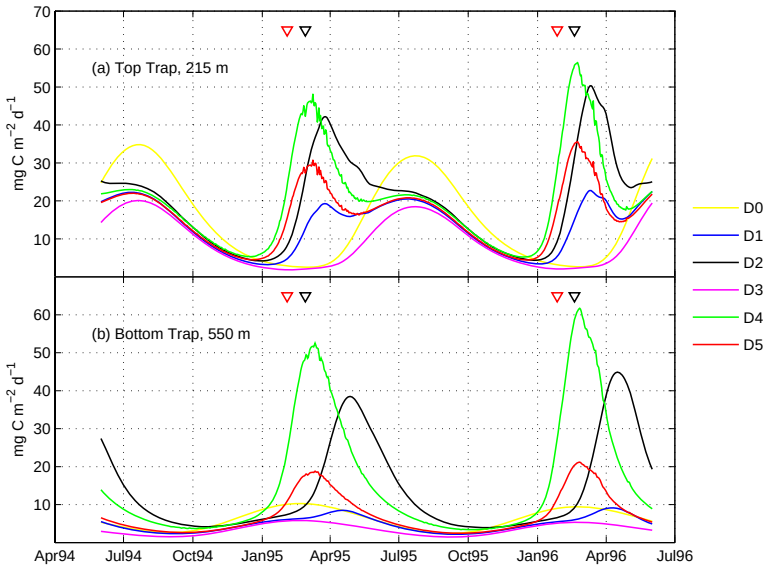

Fig. 11. Sensitivity analysis on the simulated fluxes at the sediment traps **(a)** top and **(b)** bottom. The red and blue triangles mark the peaks of surface production and biomass for each year, respectively. Experiment details are given in Table 1.